MJFAS MALAYSIAN JOURNAL OF FUNDAMENTAL AND APPLIED SCIENCES
PRINT ISSN: 2289-5981 | ONLINE ISSN: 2289-599X

RESEARCH ARTICLE

Enhanced gas separation performance of polysulfone membrane by incorporation of zeolite-templated carbon

Rika Wijiyanti [a], Anggita Rara Kumala Wardhani [a], Rosyiela Azwa Roslan [b, c], Triyanda Gunawan [a], Zulhairun Abdul Karim [b, c], Ahmad Fauzi Ismail [b, c], Nurul Widiastuti [a,*]

[a] *Department of Chemistry, Faculty of Science, Institut Teknologi Sepuluh Nopember, Sukolilo, Surabaya 60111, Indonesia*
[b] *Advanced Membrane Technology Research Center (AMTEC), Universiti Teknologi Malaysia, 81310 UTM Johor Bahru, Johor, Malaysia*
[c] *Department of Energy Engineering, School of Chemical and Energy Engineering, Universiti Teknologi Malaysia, 81310 UTM Johor Bahru, Johor, Malaysia*

* *Corresponding author: nurul_widiastuti@chem.its.ac.id*

Article history
Received 7 Mac 2019
Revised 10 May 2019
Accepted 25 July 2019
Published Online 15 April 2020

Graphical abstract

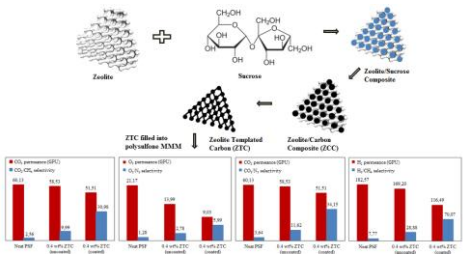

Abstract

The zeolite-templated carbon (ZTC) with a unique structure was utilized as a new porous filler for preparing mixed matrix membrane (MMM). The zeolite-Y used as template was synthesized via hydrothermal method. The ZTC was prepared by impregnation of sucrose into the pore of zeolite-Y, followed by carbonization and template removal. The obtained ZTC was characterized by X-ray diffraction (XRD), scanning electron microscopy (SEM) and N_2 isotherm analysis. Results showed that the ZTC was amorphous and possess specific surface area of 1254 m^2/g and 0.95 cm^3/g for total pore volume. The MMM was fabricated by adding 0.4 wt% ZTC via dry/wet spinning process with polysulfone (PSF) as the matrix. The fabricated membranes were analyzed using Fourier transform infrared spectroscopy (FTIR), scanning electron microscopy (SEM), atomic force microscopy (AFM), and thermal gravimetric analysis (TGA), whereas the gas permeation properties were tested using single gases (CO_2, O_2, N_2, CH_4, and H_2). The SEM results showed that incorporation of the ZTC was found to be similar as the morphological structure (dense layer and finger-like structure) of neat PSF membrane and the thermal stability was observed to be enhanced. In comparison to neat PSF membrane, uncoated PSF/ZTC MMM exhibited selectivities improvement for CO_2/CH_4 (290%), O_2/N_2 (117%), CO_2/N_2 (219%) and H_2/CH_4 (272%), while coated PSF/ZTC MMM showed enhancement up to 1110%, 368%, 838%, and 802%, respectively with acceptable permeances. Compared to neat PSF membrane, profound selectivities enhancement could be achieved even with low ZTC loading inside the MMM.

***Keywords*:** Mixed matrix membrane, zeolite templated carbon, gas separation

INTRODUCTION

Nowadays, membrane is widely used for gas separation due to its myriads of benefits, including low energy requirement, ease in operation without moving parts, and easy to scale up (Yeo *et al.*, 2012). At first, polymeric membranes have been reported for some industrial application, such as acid gases removal from natural gas, nitrogen or oxygen enrichment from air, and hydrogen recovery from hydrocarbon (Bernardo and Clarizia, 2013). In terms of industrial purpose, polysulfone exhibits potential combination between gas permeability and high intrinsic selectivity coupled with good mechanical and thermal properties, ease of fabrication, and commercial availability (Zornoza *et al.*, 2011). However, the performance of polymeric membranes is hard to achieve profound improvement. On the other hand, attempts to enhance the permeability usually results in loss in selectivity and vice versa. Therefore, development of polymeric membrane is crucial to enhance its performance.

Several researchers have developed composite membrane by incorporating adsorptive and diffusive properties of inorganic filler into the polymer matrix, known as mixed matrix membrane (MMM). The combination between two materials offers a better membrane by allowing simultaneous integration of polymer's ease processability and good performance of inorganic fillers (Dong *et al.*, 2013). As a result, an improvement in selectivity can be achieved with slight reduction in permeance.

The performance of inorganic filler is greatly depending on the filler choice. Many porous inorganic fillers such as zeolites (Junaidi *et al.*, 2015), carbon molecular sieves (Wiryoatmojo *et al.*, 2015), and carbon nanotubes (Kim *et al.*, 2007) have been proven to give different performance on gas separation properties. Zeolite-templated carbon (ZTC) is one of the porous filler with negative replica structure of zeolite template which can be produced by simple impregnation method. Although the ZTC is well-known for its excellent structure such as high surface area, high total pore volume, and ordered pore structure, this material has not been reported yet for gas separation membrane (Nishihara and Kyotani, 2012). However, the ZTC has

been proven to be suitable as adsorbents for methane, carbon dioxide, and hydrogen due to its adsorptive capability (Antoniou *et al.*, 2014; Nishihara *et al.*, 2009; Xia *et al.*, 2011). Thus, this material fits to the required characteristics for gas separation membrane.

This study aimed to enhance the performance of PSF hollow fiber membrane by incorporating ZTC as nanoporous filler. The effects of the ZTC content on membrane morphological and thermal properties as well as gas transport properties were reported.

EXPERIMENTAL

Materials

Sodium aluminate powder ($NaAlO_2$, Sigma-Aldrich), sodium silicate solution (Na_2SiO_3, Sigma-Aldrich), sodium hydroxide (NaOH, Merck, 99%), and deionized water were used as the materials for zeolite-Y. Sucrose ($C_{12}H_{22}O_{11}$, Fluka, 98%), sulfuric acid (H_2SO_4, 98% pa), fluoric acid (HF, Merck, 48%), hydrochloric acid (HCl, SAP, 37%), deionized water, and nitrogen gas (N_2, 99.999%) were used to synthesize ZTC. Polysulfone (Udel PSF P-3500, Amoco chemicals), *N*,*N*-dimethylacetamide (DMAc, Merck, 99%), tetrahydrofuran (THF, QreC, 99.8%), and ethanol (EtOH, Merck) were used as the polymer matrix, non volatile and volatile solvents, as well as non solvent of membrane, respectively. The organic solvent, *N*-Methyl-2-pyrrolidone (NMP, QreC) and methanol (MeOH, Merck, 99.9%) were used as bore liquid coagulant and membrane post treatment, respectively. Polydimethylsiloxane (PDMS, Sylgard® 184, Dow Corning) and *n*-hexane were used as coating material and solvent, respectively for coating solution. All pure gases (CO_2, CH_4, O_2, N_2 and H_2, Mega Mount Industrial Gases Sdn. Bhd. Malaysia, 99.99%) were used for gas permeation testing.

Synthesis of zeolite templated carbon

The ZTC was prepared using the as-synthesized zeolite-Y template and sucrose as the carbon source via impregnation method, carbonization, and template removal.

The zeolite-Y was synthesized via hydrothermal method containing three types of gel, namely seed, feedstock, and overall gel (Mintova and Barrier, 2016). The molar ratio of feedstock gel to seed gel was 18. The seed gel was prepared by dissolving NaOH in deionized water, followed the addition of $NaAlO_2$ and stirring until homogeneous solution. The similar step was conducted for preparing the feedstock gel. Then, the seed gel was mixed into the feedstock gel to form the overall gel and stirred until homogeneous. The obtained gel was aged for 24 h and subjected to the hydrothermal reaction at 100 °C for 7 h in autoclave. The wet zeolite-Y was filtered and washed with deionized water to get pH 8, then dried at 110 °C for 12 h. Before being used as a template, the obtained zeolite-Y was degassed at 200 °C for 4 h under N_2 flowing to remove adsorbed water.

The treated zeolite-Y was then added into the sucrose solution (sucrose in 0.35 M H_2SO_4) and stirred for 72 h in room temperature. The mass ratio of sucrose and zeolite-Y was 1.25:1. The obtained solution was filtered and its residue was placed in tubular holder, then subjected to carbonization process. The carbonization treatment was conducted in a tubular furnace at temperature of 800 °C for 4 h and a heating rate of 2 °C/min under N_2 flowing. Subsequently, the sample was cooled until room temperature under N_2 stream, followed by treating with strong acid solution to remove the zeolite-Y template. First, the composite product was immersed in 5% HF solution for 1 h to break the silica bonding, then filtered and washed with deionized water to get neutral pH of filtrate. This was followed by drying at 110 °C for 12 h. Then, the sample was refluxed in concentrated HCl at 60 °C for 1 h to remove the aluminium from zeolite-Y framework, and followed by filtering, washing with deionized water until neutral pH, and drying at 120 °C for 12 h. Lastly, the sample was soaked in 48% HF solution for 1 h to completely release the zeolite framework content. The treated sample was then filtered and washed with deionized water repeatedly until pH 7, followed by drying at 120 °C for 12 h. The ZTC was obtained in form of black residue. The ZTC was sieved to get a fine particles and dried in an oven for at least 24 h at 80 °C to release adsorbed water prior to use.

Fabrication of hollow fiber membranes

The dope solution consisted of 30 wt% PSF, 30 wt% DMAc, 30 wt% THF, and 10 wt% EtOH. Prior to use, PSF was dried at 80 °C for at least 24 h. The amount of ZTC filler added was 0.4 wt% in the total solid. The dope solution was prepared according to the following procedure.

A certain amount of the ZTC was dispersed in DMAc and ultrasonicated. Then, THF was poured into the suspension and sonicated to obtain better dispersion. About 10 wt% (10 g) of PSF was added to the mixture solution and stirred, followed by adding the remaining PSF gradually. The mixture was kept under stirring until homogeneous solution was obtained. Subsequently, ethanol was added dropwise to the solution under rigorous stirring. The dope solution was then sonicated for 1 h and kept for 24 h to remove any bubbles.

The dope solution was moved into the dope reservoir and connected to the spinneret (OD/ID: 0.8/0.4 nm). The dope flow rate was 1 ml/min. A mixture of 90 wt% NMP/10 wt% distilled water as bore coagulant was connected to the spinneret with flow rate of 0.7 ml/min. The nascent fibers passed through the dry gap of 4 cm in height. Then, the fibers were passed through the external coagulant (tap water) and collected using spinning drum at a speed of 10 m/min. After spinning, the fibers were immersed in tap water for 48 h to release the remaining solvent, followed the solvent exchange treatment by immersing the fibers in methanol over 4 h. Afterward, the obtained fibers were dried at room temperature for 48 h.

Single gas permeation test

The fiber that has been treated was potted into the lab scale module. Each module consisted of five fibers with length around 20 cm. The potted fibers before and after surface coating in 3 wt% PDMS in *n*-hexane were tested for pure gases (CO_2, O_2, CH_4, N_2, and H_2) at room temperature and pressure of 5 bar. The gas permeation test was performed using single gas permeation testing system, as shown in Fig. 1. The flux of gas *i* was obtained according to Eq. (1)

$$P_i/l = Q_i/A\ \Delta P \qquad (1)$$

where P_i/l is the flux of gas *i* across the membrane (1 GPU = $1x10^{-6}$ cm^3 (STP) / cm^2 s cm Hg), Q_i is the volumetric flow rate of permeation gas *i* through the membrane (cm^3/s, STP), *A* is the effective membrane area (cm^2), and ΔP is the pressure difference (cmHg). The permeability in Barrer unit was also determined by using an average skin layer thickness as calculated using Eq. (2). It was assumed that the thickness of all membranes were similar because they were fabricated under the same conditions (Zulhairun *et al.*, 2015).

$$l = P_i / (P_i/l) \qquad (2)$$

The ideal gas selectivities were determined by taking the ratio of fluxes. The flux and selectivity values were reported from the average of at least 3 replicated modules.

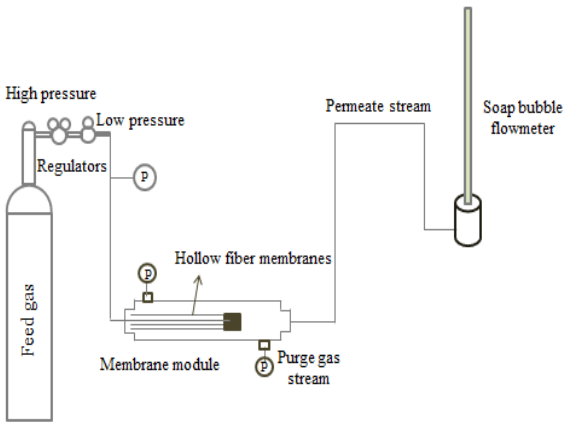

Fig. 1 Gas permeation testing rig.

Characterizations

The crystal phase of the zeolite-Y and the ZTC was examined using X-ray diffraction (Expert PAN Analytical). The pore properties of the ZTC were analyzed using surface area and porosity analyzer (Micromeritics, ASAP 2020 V4.02). The specific surface area was calculated using Brunauer-Emmet-Teller (BET) method, while the total pore volume was determined using the amount of N_2 adsorbed. The pore size distribution of the ZTC was determined via NLDFT method (a method included in the SAEIUS software of Micromeritics) with the assumption of slit pore geometry. Prior to analysis, the sample was degassed at 250 °C for 12 h under vacuum condition. The zeolite-Y and ZTC morphologies were examined using scanning electron microscope (SEM, ZEISS EVO MA 10). The membrane morphology was examined using tabletop scanning electron microscope (SEM, Hitachi TM3000). Before analysis, a piece of fiber was immersed in liquid nitrogen and cut to get a smooth cross section. Thermal stability of membranes was examined using thermogravimetry analyzer (Mettler Toledo TGA/SDTA851^e). Temperature used for analysis was 30–800 °C with a heating rate of 10 °C/min. Functional groups of the membrane were identified using Fourier transform infrared spectroscopy (FTIR, Thermo Scientific Nicolet iS10). The obtained spectrum was used to analyze the difference in the chemical structure between neat PSF and PSF/ZTC composite membrane. The surface roughness of membranes was observed using atomic force microscope (AIST-NT, Inc.).

RESULTS AND DISCUSSION

Characterization of the particles

XRD analysis

Fig. 2 shows the XRD spectrum of the zeolite-Y standard, as-synthesized zeolite-Y, and ZTC particles. Fig. 2a shows the appearance of many sharp peaks due to the topology structure of zeolite-Y framework. All spectrums were in good accordance with the standard's peaks of JCPDS no:39-1380. Among of them, the sharpest peak at 2θ = ~6° corresponds to the diffraction of (111) plane. The XRD pattern of ZTC (Fig. 2b) shows diffraction peaks at 6.05° with a broad and weak peak at ~20-27°. The appearence of peak at ~6° suggests that there was ordering structure of sample from (111) peak of zeolite template (Nishihara and Kyotani, 2012). However, the presence of a broad peak at ~20-27° indicates that ZTC was in amorphous phase. These peak can be characterized as the diffraction of (002) plane from low cristallinity of graphitic carbon (Ma *et al.*, 2000). The formation of graphitic carbon may occured due to the presence of stacking graphene on the external surface of zeolite, indicating an incomplete filling of zeolite pores by the carbon. These observation lead to the conclusion that the ZTC possesses some pore structure ordering of template and also graphitic carbon.

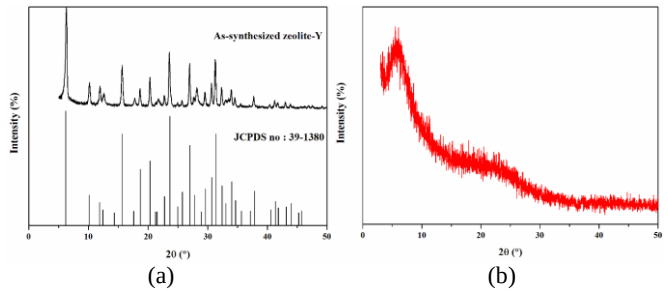

(a) (b)

Fig. 2 X-ray diffraction spectra of (a) prepared zeolite-Y template with the standard and (b) ZTC.

SEM analysis

The morphology of zeolite-Y (Fig. 3a) exhibits an octahedral crystal from each particles, as observed in literature (Nishihara and Kyotani, 2012). This result suggests that zeolite-Y synthesized from $NaOH$-$NaAlO_2$-Na_2SiO_3-H_2O system was well-formed with an average particle size of 1129 nm. Fig. 3b reveals that ZTC is a partially replicated octahedral crystal of zeolite Y template with a few aggregates of amorphous carbon. This indicates that ZTC could not preserve the morphology of zeolite-Y, which was in agreement with XRD result. Furthermore, the particle size of ZTC particles was in the range of 200–400 nm, smaller than those of zeolite-Y. The reduction in particle size might be due to the particle shrinkage during carbonization treatment which is probably ascribed to the shrinkage of zeolite-Y framework and/or carbon (Su *et al.*, 2004).

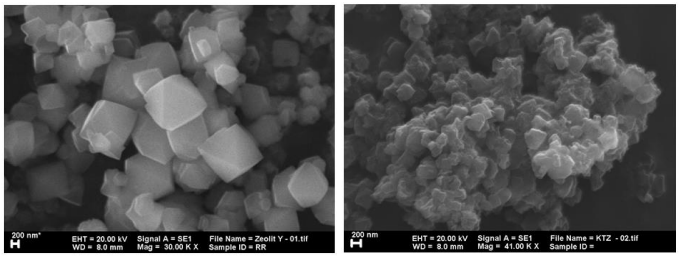

(a) (b)

Fig. 3 SEM images of (a) zeolite-Y and (b) ZTC.

BET analysis

The surface area of the ZTC determined using BET method was 1254 m^2/g. The surface area obtained in this work was comparable with the values published for ZTC sample (Konwar and De, 2014; Song *et al.*, 2013). A higher surface area may enhance sorption capacity of gases. As a result, a higher gas permeance is supposed for membrane filled using large surface area of particle (Zulhairun *et al.*, 2017). Fig. 4 shows that ZTC possesses micro and mesoporous structure ($4 < d_p < 150$ Å) with a mean pore size of 15 Å and a total pore volume of 0.95 cm^3/g. A fine pore size distribution of filler may increase gas permeability of membrane (Dong *et al.*, 2013). The presence of mesopores in ZTC sample may be due to the shrinkage of zeolite or carbon during carbonization and/or incomplete filling of the zeolite channels and cavities, as explained in XRD and SEM result (Su *et al.*, 2004).

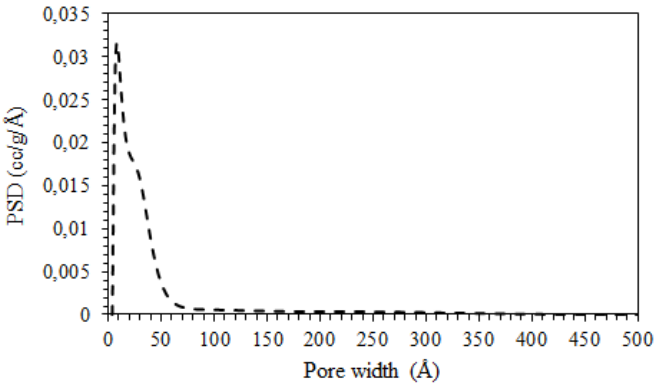

Fig. 4 Pore size distribution of the ZTC with NLDFT method.

Characterization of membranes

Structural analysis of membrane

In order to evaluate the interaction between PSF and ZTC, the FTIR spectra of neat PSF and MMM were recorded. Fig. 5 exhibits the FTIR spectra of prepared membranes. In the neat PSF spectrum, there are some peaks at 852 and 872 cm^{-1} corresponding to C-H rocking. The peaks occuring at 1013, 1079, 1104, and 1168 cm^{-1} correspond to the C-C stretching, while the peaks at 1148 and 1322 cm^{-1} are characteristic of Ar-SO_2-Ar asymmetric stretching. Furthermore, the bands at 1236 and 1293 cm^{-1} signify the Ar-O-Ar and S=O stretching, respectively, while the strong band at 1583 cm^{-1} indicates the presence of C=C aromatic stretching. All spectra pattern are similar to that observed in literature for PSF membrane (Singh *et al.*, 2014). The similar absorbance of neat PSF membrane were observed in the MMM, supporting the existance of polysulfone as

matrix. Furthermore, the occurance of new peaks or wavenumber shift are not observed for PSF membrane with ZTC adding. This observation suggests no bonds between PSF chains and ZTC functional groups.

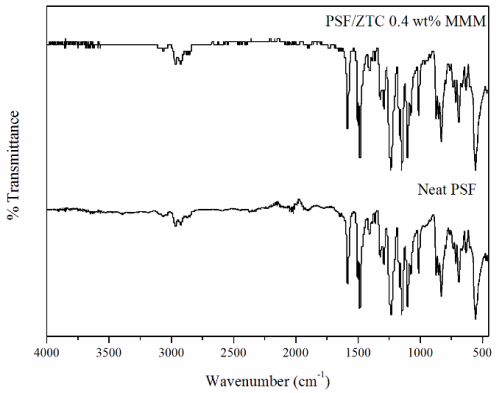

Fig. 5 FTIR of neat PSF and PSF/ZTC MMM.

Morphological analysis of membrane

In order to assess the ZTC dispersion inside the PSF matrix, the membranes were subjected to SEM analysis. The surface and cross sectional images for neat PSF and MMM are shown in Fig. 6. According to Fig. 6a1, no voids or defects were observed in the dense selective layer of neat PSF membrane and the layer thickness was about 117 nm. Conversely, Fig. 6b1 demonstrates the existence of pinholes or defects due to the particles assembled. The presence of voids suggests low interfacial adhesion between polymer matrix and ZTC surface.

As shown in Fig. 6(a2 and b2), all prepared membranes reveal asymmetric structure, i.e. dense layer on the top and porous layer on the bottom of membrane. The presence of THF in the dope solution leads to a delayed demixing, thus resulting in a porous membrane structure under the skin outer layer. Similar asymmetric structure of composite membrane was also investigated in the previous study (Zulhairun *et al.*, 2017). However, the agglomerated ZTC was observed for composite membrane with diameter of particles ranging from 1–2.6 µm. The ZTC particles were easily interacted to each other due to poor interaction between ZTC and PSF matrix, as observed from FTIR result. This leads to the formation of voids on the surface of membrane.

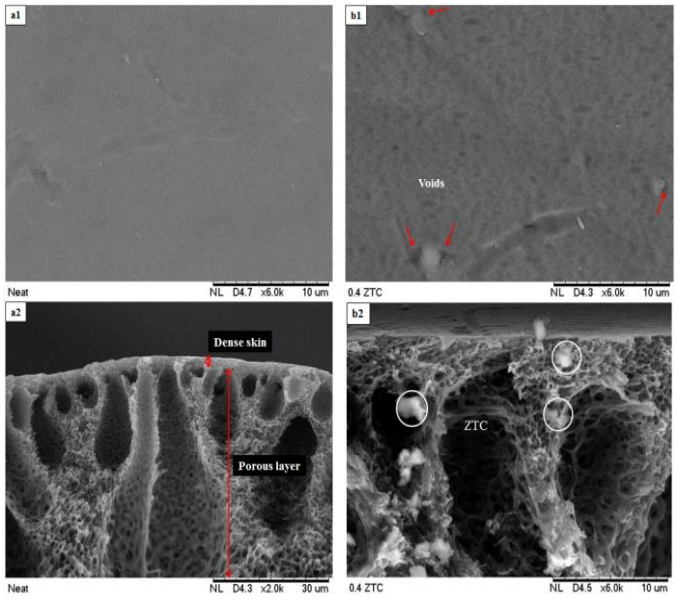

Fig. 6 SEM micrographs for surface (upper) and cross section (bottom) of (a) neat PSF and (b) PSF/ZCT 0.4% membrane.

Topology analysis

The plane and three-dimensional AFM images of all fabricated membranes are shown in Fig. 7. According to the image, the surface of neat PSF membrane was relatively smooth. However, the membrane surface roughness changes during the adding of 0.4 wt% ZTC. The addition of ZTC increased the valley and nodule of membrane, thus increasing the surface roughness of MMM. The roughness parameter of the membrane are listed in Table 1. This results are in well agreement with SEM analysis. Furthermore, the AFM image of MMM confirms that the ZTC was well-embedded on the membrane surface. For the image of MMM, the darker and brighter color signify the presence of polysulfone matrix and ZTC filler region, respectively. This observation was also observed previously (Goh *et al.*, 2011).

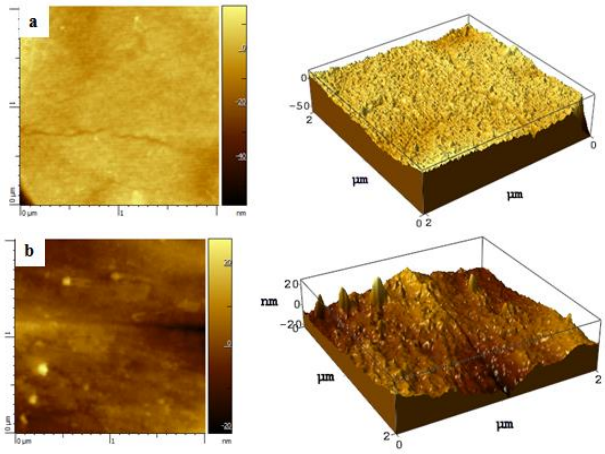

Fig. 7 The AFM images of (a) neat PSF and (b) PSF/ZTC membranes.

Table 1 Surface roughness parameter of membranes.

Membrane	Ra (nm)	RMS (nm)
Neat PSF	2.88	4.23
PSF/ZTC 0.4 wt%	3.36	4.51

Thermal analysis of membrane

The results of TGA analysis for neat PSF and PSF/ZTC composite membrane are reported in Fig. 8. The pure PSF membrane started to decompose at 120 °C, indicating the evaporation of remaining solvent, then followed by ~64% weight loss of the polymer decomposition at temperature of ~500 °C. On the other hand, the initial decomposition temperature of MMM increases to ~509 °C with a major weight loss of ~62%. In addition, a further degradation of the residue occurs for all membranes at about 550 °C. However, the residue of the MMM at temperature of 800 °C is 7.2% higher if compared to neat PSF membrane. The results demonstrate that the thermal stability of membrane is enhanced in the presence of ZTC. Similar pattern have been investigated for other polysulfone based membrane (Zulhairun *et al.*, 2017).

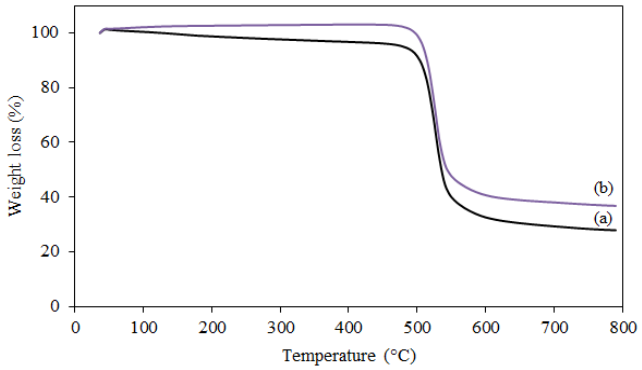

Fig. 8 TGA curve of (a) neat PSF and (b) PSF/ZTC MMM.

Table 2 Gas separation performance of all prepared membranes and comparison with other polysulfone composite membranes.

Samples	Membrane performances							References
	P_{CO2}	P_{O2}	P_{H2}	$\alpha_{CO2/CH4}$	$\alpha_{O2/N2}$	$\alpha_{H2/CH4}$	$\alpha_{CO2/N2}$	
Neat PSF	7.04	2.48	21.36	2.56	1.28	7.77	3.64	This work[a]
	60.13	21.17	182.57	2.56	1.28	7.77	3.64	This work[b]
PSF/ZTC 0.4 wt% (uncoated)	6.85	1.64	19.80	9.99	2.78	28.88	11.62	This work[a]
	58.53	13.99	169.20	9.99	2.78	28.88	11.62	This work[b]
PSF/ZTC 0.4 wt% (coated)	6.03	1.06	13.63	30.98	5.99	70.07	34.15	This work[a]
	51.51	9.03	116.49	30.98	5.99	70.07	34.15	This work[b]
Neat PSF	187	135	-	1.02	1.00	-	1.40	(Magueijo *et al.*, 2013)[b]
PSF/carbon xerogel 5 wt%	262	175	-	1.20	1.13	-	1.68	(Magueijo *et al.*, 2013)[b]
Neat PSF	0.50	0.25		2.00	0.71		1.43	(Kiadehi *et al.*, 2014)[b]
PSF/F-TiO_2 10 wt%	3.40	1.10	-	4.38	1.60	-	5.07	(Kiadehi *et al.*, 2014)[b]
Knudsen selectivity[c]				0.60	0.94	2.82	0.80	

[a]*P* in Barrer unit (1 Barrer = $1x10^{-10}$ cm^3 cm/cm^2 s cm Hg).

[b]*P* in GPU unit (1 GPU = $1X10^{-6}$ cm^3/cm^2 s cm Hg).

[c]Measured using equation in the literature (Weigelt *et al.*, 2018).

Gas permeation properties of membrane

In order to examine the effect of ZTC loading on the gas separation performance of PSF membrane, the pure gas separation experiment was performed. Table 2 and Fig. 9 present the effects of ZTC incorporation into PSF membrane on the gas permeation properties. Based on a previous study, the ZTC have been used for hydrogen and carbon dioxide adsorbent regarding to its ordered pore structure, uniform pore size, and high physisorption properties towards CO_2 and H_2 gases (Nishihara and Kyotani, 2018). This work exhibits that addition of 0.4 wt% ZTC into PSF resulted in significant enhancement in CO_2/CH_4, O_2/N_2, CO_2/N_2, and H_2/CH_4 selectivities by 290%, 117%, 219%, and 272%, respectively, compared to the neat PSF membrane. The improvement in selectivities may not be due to molecular sieving mechanism, because the average pore size of ZTC (15 Å) is bigger compared to the molecular diameter of gases. Furthermore, the selectivities enhancement cannot be explained by Knudsen diffusion mechanism, which is governed by the voids since the calculated Knudsen selectivity values (Table 2) were not in agreement with the experimental selectivity values (Weigelt *et al.*, 2018). This indicates that the gas transmission mechanism of membranes is still dominated by solution diffusion mechanism of polysulfone matrix and the contribution of the ZTC filler. The results suggest that the transport mechanism through the ZTC can be attributed to surface diffusion mechanism with a preferential surface flux of more adsorbable gases (CO_2, O_2, and H_2) over the less adsorbable gases (CH_4 and N_2) (Anson *et al.*, 2004). However, the permeability of membrane is slightly reduced in the presence of ZTC. The decreasing in permeability might be attributed with a reduction of polymer chain mobility, thus obstructing the gas to diffuse easily.

Furthermore, the MMM was coated using PDMS coating solution in order to minimize the active layer defects. As expected, the permeances of the slower and larger kinetic diameter gases were significantly reduced, which resulted high improvement in selectivities. Table 2 also exhibits the comparison of gas separation performance for other PSF composite membranes. It is worthwhile to note that a lower percentage of ZTC loading gives higher selectivities improvement as compared to other studies which incorporated higher inorganic loadings. As shown in Fig. 10, all prepared membranes in this work were still located below the Robeson upper bound 2008. However, the membrane performance was shifted toward the upper bound and showed good increment upon the addition of ZTC. The membrane performance can be further enhanced by improving the compatibility between PSF and particles through an ongoing investigation.

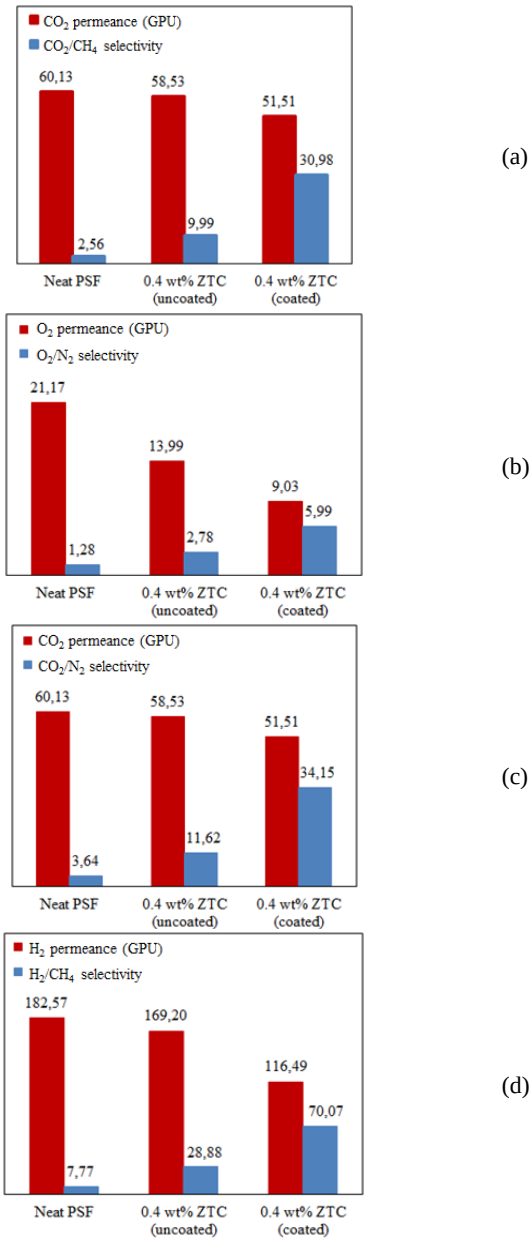

Fig. 9 Gas separation performance of membrane for (a) CO_2/CH_4, (b) O_2/N_2, (c) CO_2/N_2 and (d) H_2/CH_4 separation.

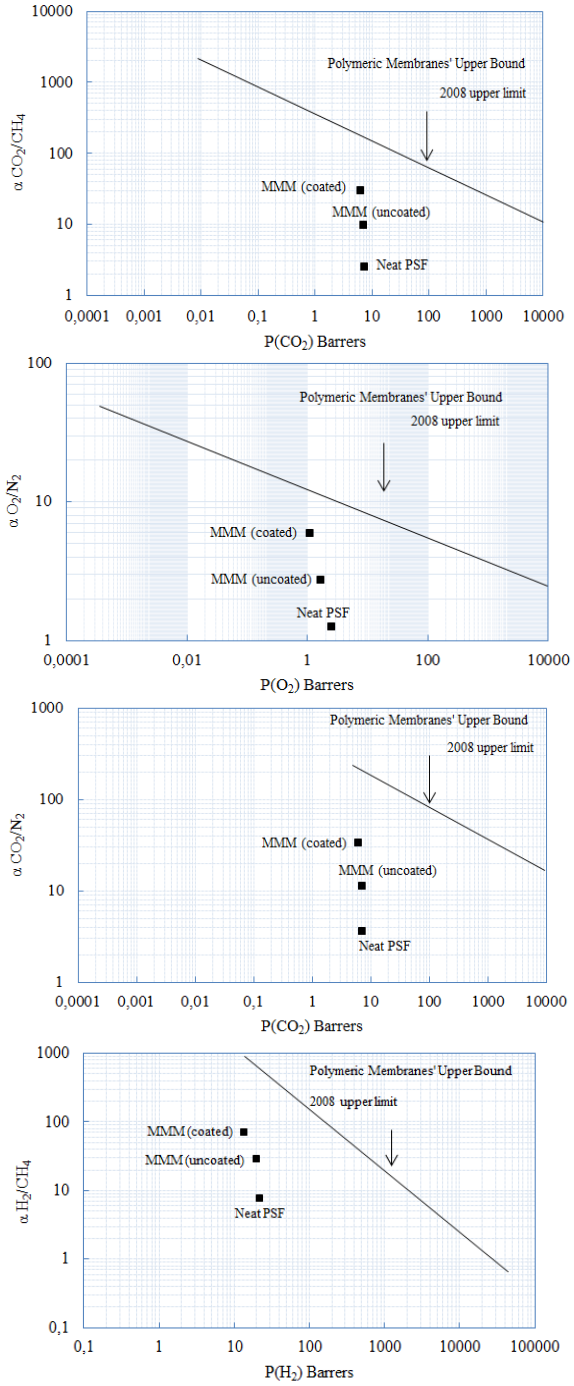

Fig. 10 The membrane performance for CO_2/CH_4, O_2/N_2, CO_2/N_2, and H_2/CH_4 toward Robeson upper bound 2008.

CONCLUSION

PSF/ZTC hollow fiber membrane was successfully fabricated. The characteristics of the ZTC and membranes in terms of structure and morphological properties, thermal stability, as well as single gas separation performance were studied. The addition of low ZTC loading into polysulfone membrane gave significant improvement for all separation even at low interaction between polysulfone and ZTC. The ZTC properties that possess high affinity toward selective gases (CO_2, O_2, and H_2) help in enhancing the membrane selectivities with significant improvement in CO_2/CH_4, O_2/N_2, CO_2/N_2, and H_2/CH_4 by 290%, 117%, 219%, and 272%, respectively, as compared to neat PSF membrane. Interestingly, coated MMM exhibited strong increase in CO_2/CH_4, O_2/N_2, CO_2/N_2, and H_2/CH_4 selectivity up to 210%, 115%, 194%, and 143%, respectively, with respect to the uncoated MMM.

ACKNOWLEDGEMENT

The authors would like to thank the Directorate General of Higher Education, Ministry of Research, Technology and Higher Education of Republik Indonesia for providing research funding under PMDSU contract no:135/SP2H/LT/DPRM/IV/2017 and PMDSU scholarship for Rika Wijiyanti to pursue Doctoral degree.

REFERENCES

Anson, M., Garis, E., Marchese, J., Ochoa, N. 2004. ABS copolymer-activated carbon mixed matrix membranes for CO_2/CH_4 separation, 243(1-2), pp.19–28.

Antoniou, M. K., Diamanti, E. K., Enotiadis, A., Policicchio, A., Dimos, K., Ciuchi, F., Maccallini, E., Gournis, D., Agostino, R. G. 2014. Methane storage in zeolite-like carbon materials. *Microporous and Mesoporous Materials*, 188, pp.16–22.

Bernardo, P., Clarizia, G., 2013. 30 Years of Membrane Technology for Gas Separation. *Icheap-11: 11th International Conference on Chemical and Process Engineering, Pts 1-4*, 32, pp.1999–2004.

Dong, G., Li, H., Chen, V., 2013. Challenges and opportunities for mixed-matrix membranes for gas separation. *Journal of Materials Chemistry A*, 1(15), pp.4610–4630.

Goh, P. S., Ng, B. C., Ismail, A. F., Sanip, S. M., Aziz, M., Kassim, M. A. 2011. Effect of dispersed multi-walled carbon nanotubes on mixed matrix membrane for O_2/N_2 separation. *Separation Science and Technology*, 46(8), pp.1250–1261.

Junaidi, M. U. M., Leo, C. P., Ahmad, A. L., Ahmad, N. A., 2015. Fluorocarbon functionalized SAPO-34 zeolite incorporated in asymmetric mixed matrix membranes for carbon dioxide separation in wet gases. *Microporous and Mesoporous Materials*, 206(C), pp.23–33.

Kiadehi, A. D., Jahanshahi, M., Rahimpour, A., Ghoreyshi, A. A., 2014. Fabrication and evaluation of functionalized nano-titanium membranes for gas separation. *Iranian Journal of Chemical Engineering*, 11(4), pp.40–49.

Kim, S., Chen, L., Johnson, J. K., Marand, E., 2007. *Polysulfone and functionalized Carbon Nanotube Mixed Matrix Membranes for Gas Separation: Theory and Experiment*, 294, pp.147–158. United States: CRC Press.

Konwar, R. J., De, M., 2012. Development of templated carbon by carbonisation of sucrose-zeolite composite for hydrogen storage. *International Journal of Energy Research*, 39, pp 223-233.

Ma, Z., Kyotani, T., Tomita, A., 2000. Preparation of a high surface area microporous carbon having the structural regularity of Y zeolite. *Chemical Communications*, pp.2365–2366.

Magueijo, V. M., Anderson, L. G., Fletcher, A. J., Shilton, S. J., 2013. Polysulfone mixed matrix gas separation hollow fibre membranes filled with polymer and carbon xerogels. *Chemical Engineering Science*, 92, pp.13–20.

Mintova, S., Barrier, N., 2016. *Verified syntheses of zeolitic materials. 3rd Revised Edition*, p. 178-180. France: Synthesis Commission of the International Zeolite Association.

Nishihara, H., Hou, P.-X., Li, L.-X., Ito, M., Uchiyama, M., Kaburagi, T., Ikura, A., Katamura, J., Kawarada, T., Mizuuchi, K., Kyotani, T. 2009. High-pressure hydrogen storage in zeolite-templated carbon. *Journal of Physical Chemistry C*, 113(8), pp.3189–3196.

Nishihara, H., Kyotani, T., 2012. Zeolite-templated carbon-its unique characteristics and applications. *Novel Carbon Adsorbents*, pp. 295-322.

Singh, K., Devi, S., Bajaj, H. C., Ingole, P., Chodhari, J., Bhrambhatt, H. 2014. Optical resolution of racemic mixtures of amino acids through nanofiltration membrane process. *Separation Science and Technology*, 49(17), pp.2630–2641.

Song, X. H., Xu, R., Wang, K., 2013. The structural development of zeolite-templated carbon under pyrolysis. *Journal of Analytical and Applied Pyrolysis*, 100, pp.153–157.

Su, F., Zhao, X. S., Lv, L., Zhou, Z., 2004. Synthesis and characterization of microporous carbons templated by ammonium-form zeolite Y. *Carbon*, 42(14), pp.2821–2831.

Weigelt, F., Georgopanos, P., Shishatskiy, S., Filiz, V., Brinkmann, T., Abetz, V. 2018. Development and characterization of defect-free Matrimid® mixed-matrix membranes containing activated carbon particles for gas separation. *Polymers*, 10(1), pp.51.

Wiryoatmojo, A. S., Mukhtar, H., Man, Z., 2010. Development of Polysulfone-carbon molecular sieves mixed matrix membranes for CO_2 removal from natural gas. *Chemical, Biological and Environmental Engineering - Proceedings of the International Conference on CBEE 2009*. 9-11 October. Singapore: World Scientific, pp.249–253.

Xia, Y., Mokaya, R., Walker, G. S., Zhu, Y., 2011. Superior CO_2 adsorption

capacity on N-doped, high-surface-area, microporous carbons templated from zeolite. *Advanced Energy Materials*, 1(4), pp.678–683.

Yeo, Z. Y., Chew, T. L., Zhu, P. W., Mohamed, A. R., Chai, S.-P. 2012. Conventional processes and membrane technology for carbon dioxide removal from natural gas: A review. *Journal of Natural Gas Chemistry*, 21(3), pp.282–298.

Zornoza, B., Téllez, C., Coronas, J., 2011. Mixed matrix membranes comprising glassy polymers and dispersed mesoporous silica spheres for gas separation. *Journal of Membrane Science*, 368(1–2), pp.100–109.

Zulhairun, A. K., Subramaniam, M. N., Samavati, A., Ramli, M. K. N., Krishparao, M., Goh, P. S., Ismail, A. F. 2017. High-flux polysulfone mixed matrix hollow fiber membrane incorporating mesoporous titania nanotubes for gas separation. *Separation and Purification Technology*, 180, pp.13–22.

Zulhairun, A. K., Fachrurrazi, Z. G., Nur Izwanne, M., Ismail, A. F., 2015. Asymmetric hollow fiber membrane coated with polydimethylsiloxane-metal organic framework hybrid layer for gas separation. *Separation and Purification Technology*, 146(January 2018), pp.85–93.